

DTIC FILE COPY

2

AD-A199 768

NPS-67-88-002

NAVAL POSTGRADUATE SCHOOL
Monterey, California



DTIC
ELECTE
OCT 25 1988
S H D

MEASUREMENTS OF GAS TURBINE COMBUSTOR
AND
ENGINE AUGMENTOR TUBE SOOTING CHARACTERISTICS

M.F. YOUNG, T.A. GRAFTON, H. CONNER
AND
D.W. NETZER

JULY 1988

Approved for public release; distribution unlimited.

Prepared for: Naval Air Propulsion Center
Trenton, New Jersey 08628-0176

88 1024 158

Naval Postgraduate School

Rear Admiral R. C. AUSTIN
Superintendent

HARRISON SHULL
Provost

The work reported herein was supported by the Naval Air Propulsion Center, Trenton, New Jersey, as part of the Navy Environmental Protection Technology Program.

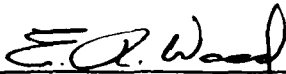
Reproduction of all or part of this report is authorized.

This report was prepared by:



DAVID W. NETZER
Professor
Dept. of Aeronautics & Astronautics

Reviewed by:



E. ROBERTS WOOD
Chairman
Dept. of Aeronautics &
Astronautics



GORDON E. SCHACHER
Dean of Science & Engineering

UNCLASSIFIED

SECURITY CLASSIFICATION OF THIS PAGE

REPORT DOCUMENTATION PAGE

1a REPORT SECURITY CLASSIFICATION UNCLASSIFIED		1b RESTRICTIVE MARKINGS	
2a SECURITY CLASSIFICATION AUTHORITY		3 DISTRIBUTION AVAILABILITY OF REPORT Approved for public release; distribution is unlimited	
2b DECLASSIFICATION/DOWNGRADING SCHEDULE			
4 PERFORMING ORGANIZATION REPORT NUMBER(S) NPS67-88-002		5 MONITORING ORGANIZATION REPORT NUMBER(S)	
5a NAME OF PERFORMING ORGANIZATION Naval Postgraduate School	6a OFFICE SYMBOL (if applicable) 67	7a NAME OF MONITORING ORGANIZATION Naval Postgraduate School	
6c ADDRESS (City, State, and ZIP Code) Monterey, California 93943-5000		7b ADDRESS (City, State, and ZIP Code) Monterey, California 93943-5000	
8a NAME OF FUNDING SPONSORING ORGANIZATION Naval Air Propulsion Center	8b OFFICE SYMBOL (if applicable)	9 PROCUREMENT INSTRUMENT IDENTIFICATION NUMBER	
8c ADDRESS (City, State, and ZIP Code) Trenton, New Jersey 08628-0176		10 SOURCE OF FUNDING NUMBERS	
		PROGRAM ELEMENT NO	PROJECT NO N62376 87WR00032
		TASK NO	WORK UNIT ACCESSION NO
11 TITLE (include Security Classification) MEASUREMENTS OF GAS TURBINE COMBUSTOR AND ENGINE AUGMENTOR TUBE SOOTING CHARACTERISTICS			
12 PERSONAL AUTHOR(S) YOUNG, M.F., GRAFTON, T. A., CONNER, H., AND NETZER, D.W.			
13a TYPE OF REPORT FINAL	13b TIME COVERED FROM OCT 86 TO SEP 87	14 DATE OF REPORT (Year, Month, Day) 1988, JULY	15 PAGE COUNT 57
16 SUPPLEMENTARY NOTATION			
17 COSAT CODES		18 SUBJECT TERMS (Continue on reverse if necessary and identify by block number)	
FIELD	GROUP	SUB-GROUP	
		Optical Sizing of Soot; Gas Turbine Combustors; Exhaust Augmentor Tubes	
19 ABSTRACT (Continue on reverse if necessary and identify by block number)			
<p>An experimental investigation was conducted to determine the changes in soot mean diameter across the combustor and exhaust nozzle of a T63 gas turbine engine, and across an exhaust augmentor tube.</p> <p>D_{32} within the combustor varied between 0.16 and 0.25 microns, depending upon fuel composition. Data correlation was most successful in this location using an index of refraction of $1.95 - 0.66i$ with $\sigma = 1.5$.</p> <p>In the aft can location (ahead of the exhaust nozzle) D_{32} was between 0.35 and 0.45 microns, depending upon the fuel-air ratio. Increasing fuel-air ratios decreased D_{32}, also in agreement with the results presented in reference 1. Both $m = 1.95 - .3i$, $\sigma = 2$, and $m = 1.95 - .66i$, $\sigma = 1.5$ could be used to successfully reduce the data.</p> <p>Using NAPC #9 high aromatic fuel, D_{32} increased across the exhaust nozzle (0.35 to 1.2 microns) and across the augmentor tube (1.2 to 1.5 to 1.9 microns). Malvern data were in good agreement with the results obtained using larger scattering angles.</p>			
20 DISTRIBUTION AVAILABILITY OF ABSTRACT <input type="checkbox"/> UNCLASSIFIED/UNLIMITED <input type="checkbox"/> SAME AS RPT <input type="checkbox"/> DTIC USERS		21 ABSTRACT SECURITY CLASSIFICATION	
22a NAME OF RESPONSIBLE INDIVIDUAL		22b TELEPHONE (include Area Code)	22c OFFICE SYMBOL

DD FORM 1473, 84 MAR

83 APR edition may be used until exhausted
All other editions are obsolete

SECURITY CLASSIFICATION OF THIS PAGE

U.S. Government Printing Office: 1986-806-24.

UNCLASSIFIED

SECURITY CLASSIFICATION OF THIS PAGE (When Data Entered)

19. ABSTRACT (continued)

The results show that significant agglomeration of the soot occurs axially within the combustor and nozzle and across the augmentor tube. These changes in soot size can have significant effects on the selection of soot reduction techniques and on the opacity of the test cell exhaust plume.



Accession For	
NTIS GRA&I	<input checked="" type="checkbox"/>
DTIC TAB	<input type="checkbox"/>
Unannounced	<input type="checkbox"/>
Justification	
By	
Distribution	
Availability	
Dis	

A-1

S/N 0102-LF-014-6601

UNCLASSIFIED

SECURITY CLASSIFICATION OF THIS PAGE (When Data Entered)

ABSTRACT

An experimental investigation was conducted to determine the changes in soot mean diameter across the combustor and exhaust nozzle of a T63 gas turbine engine, and across an exhaust augmentor tube.

D_{32} within the combustor varied between 0.16 and 0.25 microns, depending upon fuel composition. Data correlation was most successful in this location using an index of refraction of $1.95 - 0.66i$ with $\sigma = 1.5$.

In the aft can location (ahead of the exhaust nozzle) D_{32} was between 0.35 and 0.45 microns, depending upon the fuel-air ratio. Increasing fuel-air ratios decreased D_{32} , also in agreement with the results presented in reference 1. Both $m = 1.95 - .3i$, $\sigma = 2$, and $m = 1.95 - .66i$, $\sigma = 1.5$ could be used to successfully reduce the data.

Using NAPC #9 high aromatic fuel, D_{32} increased across the exhaust nozzle (0.35 to 1.2 microns) and across the augmentor tube (1.2 to 1.5 + 1.9 microns). Malvern data were in good agreement with the results obtained using larger scattering angles.

The results show that significant agglomeration of the soot occurs axially within the combustor and nozzle and across the augmentor tube. These changes in soot size cau

have significant effects on the selection of soot reduction techniques and on the opacity of the test cell exhaust plume.

TABLE OF CONTENTS

I. INTRODUCTION AND BACKGROUND 1

II. THEORY 4

 A. LIGHT TRANSMITTANCE TECHNIQUE 4

 B. FORWARD LIGHT SCATTERING TECHNIQUE 7

III. DESCRIPTION OF EXPERIMENTAL APPARATUS 9

 A. COMBUSTOR 9

 B. AIR SUPPLY 10

 C. FUEL SUPPLY 10

 D. ADDITIVE PUMPS 11

 E. THERMOCOUPLES 11

 F. AUGMENTOR TUBE 11

 G. DATA REDUCTION SYSTEM 11

 H. CONTROLS 12

 I. LIGHT TRANSMITTANCE APPARATUS 12

 J. FORWARD LIGHT SCATTERING APPARATUS 13

IV. DISCUSSION OF RESULTS 15

V. CONCLUSIONS AND PRESENT EFFORT 22

LIST OF TABLES vi

LIST OF FIGURES vii

REFERENCES 45

INITIAL DISTRIBUTION LIST 46

LIST OF TABLES

1. Properties of NAPC Fuels #2 and #9 16

LIST OF FIGURES

1. Extinction Coefficient Versus D_{32}	24
2. Extinction Coefficient Ratios Versus D_{32}	25
3. Extinction Coefficient Versus D_{32}	26
4. Extinction Coefficient Ratios Versus D_{32}	27
5. Extinction Coefficient Versus Particle Size D_{32}	28
6. Extinction Coefficient Versus Particle Size D_{32}	29
7. Intensity Ratio Versus D_{32}	30
8. Intensity Ratio Versus D_{32}	31
9. Intensity Ratio Versus D_{32}	32
10. Intensity Ratio Versus D_{32}	33
11. T-63 System Schematic [Ref. 1]	34
12. T-63 Combustor Schematic	35
13. Side View of T-63 Thermocouple Locations [Ref. 1]	36
14. End View of T-63 Thermocouple Locations [Ref. 1]	37
15. Schematic of T-63 Augmentor Tube Apparatus	38
16. Schematic of T-63 Test Apparatus (Adapted from Reference 1)	39
17. Schematic of T-63 Aft Can Transmittance Apparatus (Adapted from Reference 1)	40
18. Schematic of T-63 Combustor Transmittance and Light Scattering Apparatus (Adapted from Reference 1)	41
19. Schematic of Augmentor Tube Particle Sizing Apparatus (End View)	42
20. MALVERN Particle Size Data for Augmentor Tube Exit ...	43
21. MALVERN Particle Size Data for Exhaust Nozzle	44

I. INTRODUCTION AND BACKGROUND

At present there is a great deal of interest in the study of soot formation in gas turbine engines. In the operational environment, soot production directly affects the engine service life, reliability, and combat survivability. Soot is also one of the key contributors to the gas turbines' negative impact on environmental air quality.

Routine maintenance and overhaul of gas turbines are carried out in test cells located at various shore-based installations. These test cells are required to meet all federal standards issued by the Environmental Protection Agency concerning air pollution. The test cells must also meet any applicable local state laws which tend to be more demanding. These regulations apply to the engine when it is operating in the test cell environment, not when installed in the aircraft.

Two approaches are available for the test cells to meet their operational requirements. First, the exhaust from the test cell could be "scrubbed," but this approach tends to be prohibitively expensive if applied to all test cells. The second approach is to modify or treat the fuel with fuel additives and/or smoke suppressants, with the result being a "cleaner" exhaust product at a reasonable cost.

The objectives of current research at the Naval Post-graduate School are to determine the effects of different fuel compositions, smoke suppressants and operating conditions on:

- soot size and concentration
- NOx concentration, and
- heat release rates.

These effects are being measured both within the combustor and the exhaust augmentor tube.

This investigation was a continuation of the efforts of Bennet, et al. [Ref. 1]. A number of modifications were made to the T-63 Test Apparatus to improve the capabilities of the system. Modifications were as follows:

- Enlarging of the exhaust nozzle to meet combustor design flowrate at combustor design pressure.
- Design and installation of a rigid test stand behind the augmentor tube for accurate light scattering measurements at three forward angles.
- Installation of a smaller augmentor tube to reduce cold air induction and increase soot concentration at the exit.
- Installation of new optics and associated equipment to improve data acquisition.

The first objective of this investigation was to design and construct improvements to the transmittance and light scattering measurement equipment reported in reference 1. This was needed to increase accuracy in particle sizing in the combustor and across the augmentor tube. The second

objective was to use the apparatus to determine the changes in soot characteristics that occur from the main burner to the exhaust of the augmentor tube.

II. THEORY

There are two basic methods available for the study of the sooting characteristics in gas turbine combustors and in test cells. One approach is the withdrawal of a soot sample for analysis. These devices affect the flow process where the measurements are made. The other approach is non-intrusive, and generally utilizes measurements of scattered and/or transmitted light. This second approach was employed for the current investigation.

A. LIGHT TRANSMITTANCE TECHNIQUE

This technique incorporates the use of three different wavelengths of light for continuous transmittance measurements through a gas containing soot particles. The values of transmittance are then ratioed to each other and the particle size can then be calculated from Mie scattering theory.

This procedure was successfully applied by K. L. Cashdollar (Ref. 2) to measure the mass concentration and particle size of a cloud of smoke. The transmission of light through a cloud of uniform particles is given by reference 2:

$$T = \exp(-QAnL) = \exp[-(3QC_mL/2\rho d)] \quad (1)$$

where:

- T = fraction of light transmitted
- Q = dimensionless extinction coefficient
- A = cross-sectional area of particle
- n = concentration of particles
- L = path length of the light beam
- C_m = mass concentration of particles
- ρ = density of particles
- d = diameter of particles.

For a polydisperse system of particles, which is more characteristic of soot, Dobbins [Ref. 3] revised the above expression to the following:

$$T = \exp[-3\bar{Q}C_m L / 2\rho D_{32}] \quad (2)$$

where:

- \bar{Q} = average extinction coefficient
- D₃₂ = volume-to-surface mean particle diameter.

\bar{Q} is a function of the complex refractive index (m) of the soot, the standard deviation of the particle size distribution (σ), particle size (D₃₂), and the wavelength of the light (λ). Equation (2) can be put into a more useful format by taking the natural log of both sides.

$$\ln T = \bar{Q}[-3C_m L / 2\rho D_{32}] \quad (3)$$

Equation (3) applies to a particular wavelength (λ). The ratio of the transmittances at any two wavelengths is equal to the ratio of the calculated extinction coefficients for the same wavelengths:

$$\frac{\ln T(\lambda_1)}{\ln T(\lambda_2)} = \frac{\bar{Q}(\lambda_1)}{\bar{Q}(\lambda_2)} \quad (4)$$

The transmittances are found experimentally. A computer program provided by K. L. Cashdollar was used to generate curves for the extinction coefficient (\bar{Q}) and the extinction coefficient ratios ($\bar{Q}(\lambda_1)/\bar{Q}(\lambda_2)$) versus D_{32} . Different curves were obtained by varying the complex refractive index (m) of the soot and the standard deviation of the particle size (σ). If the complex refractive index and standard deviation were correct, all three ratios would yield the same particle size (D_{32}). If the value for D_{32} was not consistent, then either the refractive index or the standard deviation size, or both, could be varied. Using previous experience, a refractive index of $m = 1.95 - .66i$ and a standard deviation of $\sigma = 1.5$ gave the most consistent results. Figures 1 through 6 show plots from the program. It should be noted from these figures that when D_{32} is greater than approximately 0.6 microns, small errors in transmittance measurements can result in large changes in the calculated values for D_{32} .

B. FORWARD LIGHT SCATTERING TECHNIQUE

Another approach for determining the sizes of small particles is to measure the light scattered at small forward angles. Diffraction techniques alone have been shown to be quite accurate for particles as small as 0.2 microns, provided that ratioing techniques are employed. More accurate results can be obtained by using the complete Mie equations to account for diffraction, absorption and refraction. Using the diffraction technique, the ratio of intensities at two scattered angles will give a measure of the mean particle diameter. Assuming a polydisperse cloud, the ratio of intensities at any two forward scattering angles is given by the following equation:

$$I(\theta_1)/I(\theta_2) = F(\theta_1)/F(\theta_2)$$

Powell, et. al [Ref. 4] developed the following equation for $F(\theta)$:

$$F(\theta) = \int_1^2 (1+\cos^2\theta)[J_1(\alpha\theta\epsilon)/\theta\epsilon]^2 \exp[-\delta \ln(a\epsilon/1-\epsilon)]^2 d\epsilon/1-\epsilon \quad (5)$$

where:

$$\begin{aligned} \alpha &= \pi D_m / \lambda = \text{size parameter} \\ D_m / D_{32} &= 1 + (a \exp(1/4\delta^2)) \\ a &= \text{size distribution parameter} = 1.13 \\ \delta &= \text{size distribution parameter} = 1.26 \end{aligned}$$

D_m = maximum particle diameter

ϵ = particle diameter divided by D_m

J_1 = Bessel function of order one..

This equation only accounts for Fraunhofer diffraction.

Since the forward scattering lobe consists mostly of Fraunhofer diffraction, the ratio of scattered light intensities in this region is insensitive to particle refractive index and concentration (which significantly affect refraction and absorption). Using Equation 5, a plot of intensity ratios versus particle size (D_{32}) can be produced. So that the intensities are referenced to the same scattering volume, each intensity must be multiplied by the SIN of its respective scattering angle. Using this ratio as an entry to the plot, a value of D_{32} can be determined. Plots of intensity ratio versus D_{32} are presented in Figures 7-10.

III. DESCRIPTION OF EXPERIMENTAL APPARATUS

A summary of the separate pieces of equipment that make up the system is included below. Figure 11 is a schematic for the system.

A. COMBUSTOR

The combustor was the combustion section of an Allison T-63 gas turbine. The power turbine and compressor were not used. Included with the combustion can were the ignitor plug, combustor housing and the turbine nozzle block. A stainless steel exhaust chamber with converging exhaust nozzle was added aft of the turbine nozzle block to maintain the desired pressure level. Figure 12 is a schematic of the combustor.

After the first test series, several equipment modifications were made. There were two purposes for the equipment modifications. The first was to make the Allison T-63-A-5A engine, without a power turbine or compressor, perform more closely with an unmodified "in-use" turboshaft engine. The second was to modify the optics in an attempt to obtain more accurate particle sizing data.

A new heat resistant stainless steel exhaust housing, which was 15% longer than the exhaust housing used previously, was built to accommodate a quench manifold. An

additional 0.5 lbm/sec of air at approximately 40°F was supplied to the combustion section just aft of the turbine nozzle block. The purpose of the quench manifold was to better simulate an actual T-63 engine where exhaust gases from the combustor are quenched by turbine work extraction.

B. AIR SUPPLY

With the compressor removed from the combustor, air had to be supplied from a remote source. In this case, air was provided by a 3000 PSI tank storage system. This air entered into the engine through the two ducts that originally received air from the compressor.

The desired flow rates were achieved using a pressure regulator and solenoid on/off valve. A sonic choke was used together with measurements of the temperature and pressure for calculation of the flow rate.

C. FUEL SUPPLY

A hydrogen fueled air heater was installed and could be used to increase the temperature of the inlet air, if desired. Additional oxygen was added to the heated air to adjust for that consumed with the hydrogen. The ignitor and gas controls for the air heater were located in the control room.

D. ADDITIVE PUMPS

Two Eldex pumps were mounted on the test stand and were remotely operated by switches in the control room. The mixing of the fuel and the additive was done using a swirl-type mixer.

E. THERMOCOUPLES

Five thermocouples were located in the combustor. Their locations are depicted on Figures 13 and 14. The outputs of these thermocouples were monitored with a Hewlett-Packard data acquisition system.

F. AUGMENTOR TUBE

Four inch, six inch, and eight inch augmentor tubes were available for use in the experiment. Their length was six feet. The exhaust augmentation ratio is the ratio of augmentor tube suction flowrate to exhaust nozzle mass flow rate. The various sizes of augmentor tube diameters create different amounts of cold air induction. They may also result in different soot sizes at the exit, and different augmentor exhaust temperatures. A schematic of the augmentor tube is presented in Figure 15.

G. DATA REDUCTION SYSTEM

Data were recorded using a Hewlett-Packard computer system. Pressures, temperatures, flowrates, and transmittance and scattering voltages were recorded during each

portion of motor operation. The exhaust temperature of the engine was displayed on either a strip chart recorder or a digital display to determine "steady-state" for computer data acquisition and as a safety backup.

H. CONTROLS

All controls were situated such that the experiment could be run from the control room. There was a control valve for setting the desired air pressure and an electric solenoid on/off switch to initiate and terminate air flow. Controls for the fuel system included a control valve and pressure guage for the fuel tank and an electric on/off switch to control fuel flow. A flow control valve for the fuel with digital readout from the turbine flowmeter was installed adjacent to the control panel. There was also an electric vent valve to relieve pressure from the fuel tank.

I. LIGHT TRANSMITTANCE APPARATUS

Light transmittance measurements were taken at the aft end of the combustion can and in the aft pressure enclosure. In the combustion can two argon lasers and one helium-neon laser were initially used. The wavelengths for these lasers were .4880, .5145, and .6328 microns, respectively. To filter out combustion light, a light chopper on the input beams was used to provide a 90 Hz reference signal to phase-lock amplifiers, which also received the inputs from

the photodiodes. From the phase-lock amplifier the signals were sent to the computer.

As previously mentioned, light transmittance measurements were also taken in the aft pressure enclosure. A less complicated white-light source was used here since combustion light was not present. After passing through the exhaust gases the white-light was divided into three different beams using beam splitters. Each beam was passed to an individual photodiode which was preceded by a specific wavelength filter. The outputs of the three photodiodes were sent directly to the computer. The voltage signals from these diodes were also recorded on strip charts in the control room to provide a "hard-copy" of transmittance variation during an experiment. These strip charts also proved helpful in determining the proper time for computer data sampling. Figures 16, 17, and 18 show the geometry of the transmittance equipment as installed on the T-63.

J. FORWARD LIGHT SCATTERING APPARATUS

The scattered light measurement apparatus was placed at three stations on the T-63 gas turbine combustor and augmentor tube. The stations, depicted in Figure 16, were located in the combustor, and in the exhaust can. Also, measurements were made in the exit plane, immediately aft of the augmentor tube (Figure 19).

The combustor section apparatus consisted of 90 Hz chopped or unchopped .4880 micron wavelength light, provided by an argon laser and two photodiode detectors positioned at 20° and 40°, each containing a photodiode and a narrow pass, laser line filter. The .4880 micron wavelength light was chosen for the scattering measurements because it was the most powerful of the lasers available for experimental use and the majority of light generated by the combustion process was suspected to be at the higher wavelengths.

The exhaust section forward-scattering apparatus was the same as the combustor scattering apparatus except in two important areas. First, the laser light beam did not need to be chopped, and, secondly, the laser light source was supplied by a less powerful helium-neon laser.

The aft-most light scattering apparatus was located at the exit plane of the augmentor tube, Figure 19. The set-up was exactly that of the exhaust equipment, except three detector boxes were used instead of two. Initially, they were set at angles of 10°, 20°, and 40° or 10°, 20°, and 30°. Later they were changed to 5°, 10°, and 20°.

IV. DISCUSSION OF RESULTS

The initial test series consisted of four runs utilizing the T-63 data acquisition system with the instrumentation discussed above, and two additional runs using a Malvern 2600 particle sizer to verify some of the data from the first four tests. Normal test conditions were an air flow rate of 1.75 lb/sec, an air inlet temperature of 500°R and a combustion pressure of 100 psi.

All of the initial tests were made using NAPC 9 fuel (high aromatic JP-5, Table I). No additives were used, but tests were made at two different fuel-to-air ratios. The first test used a fuel-to-air ratio of .0159. All other tests were made at a higher ratio of .0179.

Data reduction for the first test yielded a particle size (D_{32}) of .45 microns in the aft can. All three transmittance ratios gave very consistent results using the MIE-SCAT program with m at 1.95 - .3i and σ set to 2.0. Very low values (less than 5%) of transmittance were obtained in the combustor. This indicated that the low fuel-to-air ratio produced an extremely soot-laden flow. No particle size could be determined.

For the first test, the augmentor scattering apparatus was configured with photodiodes at 10°, 20°, and 40°. The initial data reduction showed some scattering at 10° and 20°,

TABLE I

PROPERTIES OF NAPC FUELS #2 AND #9

	<u>NAPC #2</u>	<u>NAPC #9</u>
API Gravity @ 15°C	37.8	40.5
Distillation		
IBP °C	168	190
Recovered 10% Max	227	204
Recovered 20%	242	208
Recovered 50%	257	218
Recovered 90%	272	246
End Point, Max	281	264
Residue (ML), Max	1.8	1.4
Loss (MI), Max	0.2	0.5
Composition		
Aromatics (Vol %), Max	19.8	22.7
Olefin (Vol %), Max	0.81	1.62
Hydrogen Content (Wt %), Min	13.48	13.49
Aniline--Gravity Prod., Min	5557	5471
Freeze Point, °C	-24.0	-53.0
Viscosity @ 37.8°C (cSt)	2.27	1.50
Temperature @ 12 cSt, (°C)	-20.6	-35

but nothing at 40°. Dominant scattering at the lower angles indicated that large particles were exiting the augmentor tube. Prior to the third test, the augmentor scattering diodes were recalibrated to determine more accurate calibration constants (voltage outputs for fixed intensity input) for each diode. When the corrected calibration constants were applied to the $I(\theta = 20^\circ)/I(\theta = 10^\circ)$ raw data from the first test, a mean particle size (D_{32}) of 1.50--1.52 microns was determined.

The second and all subsequent tests were made at the fuel-air ratio of .0179. This higher ratio resulted in a particle size in the aft can of .36 microns. This decrease in D_{32} with increased fuel-air ratio was in agreement with the behavior observed by Jway, et al. [Ref. 1]. The transmittances in the combustor improved from those obtained at low fuel-air ratios, to 10.8% for the He-Ne laser and 30.6% for the argon laser. This result was inconsistent with theory, since the higher wavelength (.6328 microns) should have resulted in a higher transmittance than the lower wavelength (.488 microns).

Again, the augmentor photodiodes showed scattering at 10° and 20°, but nothing at 40°. When the data were reduced using the correct calibration constants, a particle size of 1.55 microns was obtained. This was in good agreement with the results from test one.

The third test failed to produce any accurate particle sizing data in the aft can. The transmittance values obtained for the combustor were 17.9% for the He-Ne laser and 30.5% for the argon laser, again in reverse order to what should have been observed.

The augmentor tube photodiodes were changed to 10°, 20°, and 30° in an attempt to obtain data at three angles. Again, only the 10° and 20° diodes recorded measurable intensities. This test resulted in a particle size of 1.52 microns.

It was observed in the first three tests that the high power of the argon laser, coupled with small misalignment of the windows, resulted in many reflections along the optical path through the combustor. In an attempt to see if this was the cause for the incorrect transmission intensities, a fourth test was conducted in which the higher-powered argon laser was replaced with a smaller (8 mW) argon laser. A beam splitter was also removed which increased the intensity of the He-Ne laser. The result was a transmittance of 17.3% at .6328 microns and 7.3% at .4880 microns. This result agreed with the expected behavior from scattering theory. This one ratio yielded a particle size of .15-.17 microns in the combustor for $m = 1.95 - .66i$ and $\sigma = 1.5$.

The very large D_{32} measured at the augmentor tube exhaust was not expected, thus the selection 10°, 20°, and 30° or 40° for scattering angles. For $D = 1.5$ microns, 30° is approximately the end of the Fraunhofer center lobe, where

accuracy of the theory is questionable. It was decided to use another measurement device, which used smaller angles, to check the accuracy of the approximately 1.5 microns mean size discussed above. The fifth and sixth tests were conducted using a Malvern 2600 HSD particle sizer to determine the particle size distribution at the exit of the augmentor tube and at the exit of the T-63 combustion can nozzle. No combustor data were taken during either of these runs. At the augmentor tube exit, 80% of the particles had diameters between 1.4 and 1.9 microns and D_{32} was 1.9 microns. Data from this test are included as Figure 20. This result was in good agreement with the data from the first three tests. In order to measure particles as small as 0.5 microns, the Malvern had to be operated with a 63 mm lens, the least accurate configuration. Also, the optimum condition would be for the Malvern sample volume to be within one focal length of the lens. This was not possible due to the diameter of the augmentor tube.

Data from the sixth test confirmed the particle size obtained earlier for the aft can. During this test, the Malvern was positioned to determine the particle size distribution at the exit of the exhaust nozzle (i.e., the entrance to the augmentor tube). The result was that 10% of the particles had diameters between 1.4 and 1.6 microns, 42% between 1.2 and 1.4, and 41% between 0.5 and 1.2 microns. D_{32} was 1.2 microns. Data are included as Figure 21. This

indicated that the particles were agglomerating as they passed through the converging nozzle and through the augmentor tube.

The Malvern was used to verify the data that were being obtained from the three-angle measurement apparatus. In both cases, the results were in very close agreement with data from the previous runs, especially when the less than optimum operating conditions for the Malvern were taken into account. During the second test series all of the test runs were made using NAPC-2 fuel (Table I). No additives were used. The fuel-air ratio for all runs was .0180. In these tests quench air was utilized aft of the combustor to reduce the stagnation temperature before exhausting into the augmentor tube. Normal test conditions were unchanged except that 0.25 lbm/sec of quench air at 500°R was used. Based upon the large observed particle sizes at the augmentor tube exhaust during the first test series, the diode angle configuration was changed. The first eleven runs were made with the augmentor tube photodiode geometric configuration set at -5°, 10°, and 20°. The smallest angle of -5° resulted in measurements which were contaminated with light defracted from beam stops. Subsequent tests were therefore conducted using 10°, 20°, and 30° forward scattering angles. Signal to noise ratio problems existed for the 30° location. Thus, only the light scattered at 10° and 20° could be consistently used to measure particle diameter.

At the augmentor tube exhaust the mean particle diameter size was measured to be between .77 microns and .82 microns using scattered light at the 20° and 10° augmentor photodiodes. Within the combustor D_{32} was .22 -.25 microns. This resulted from using the log ratios of the .6328 and .5145 micron transmittances together with $m = 1.95 - 66i$ and $\sigma = 1.5$.

It should be reiterated that the Malvern data were used only to compare with the light scattering measurements made at larger angles. The Malvern was used in a non-optimum configuration, the measured particle sizes were at the lower limit for the system, the obscurations were quite low (less than 5%) and the number distribution (vs. volume distribution) was utilized (which has questionable accuracy).

V. CONCLUSIONS AND PRESENT EFFORT

The major purpose of the investigation was to instrument the combustor and augmentor tube and then to determine the changes in soot size across the system. The combustor and exhaust nozzle entrance sections yielded results in good agreement with earlier data [Ref. 1].

D_{32} within the combustor varied between 0.16 and 0.25 microns, depending upon fuel composition. Data correlation was most successful in this location using an index of refraction of $1.95 - 0.66i$ with $\sigma = 1.5$.

In the aft can location (ahead of the exhaust nozzle) D_{32} was between 0.35 and 0.45 microns, depending upon the fuel-air ratio. Increasing fuel-air ratios decreased D_{32} , also in agreement with the results presented in reference 1. Both $m = 1.95 - .3i$, $\sigma = 2$, and $m = 1.95 - .66i$ $\sigma = 1.5$ could be used to successfully reduce the data.

Using NAPC #9 fuel, D_{32} increased across the exhaust nozzle (0.35 to 1.2 microns) and across the augmentor tube (1.2 to 1.5 + 1.9 microns). Malvern data were in good agreement with the results obtained using larger scattering angles.

The results show that significant agglomeration of the soot occurs axially within the combustor and nozzle and across the augmentor tube. These changes in soot size can

have significant effects on the selection of soot reduction techniques and on the opacity of the test cell exhaust plume.

The above tests were conducted using essentially one test condition and one augmentor augmentation ratio. Several additional modifications have been made to improve the apparatus for the continuing investigation.

- (1) The augmentor exhaust light scattering optics have been modified to increase the light gathering capability, while at the same time narrowing the range of scattering angles detected by any one diode.
- (2) An IR He-Ne laser has been added in the combustor section in order to provide a wider range in wavelengths for the three transmittance measurements.

A test series is currently being conducted in which fuel-air ratio, augmentation ratio, air inlet temperature, and fuel composition are all variables. Two smoke suppressant additives are also being evaluated for their effects on the sooting characteristics of both the combustor and augmentor tube.

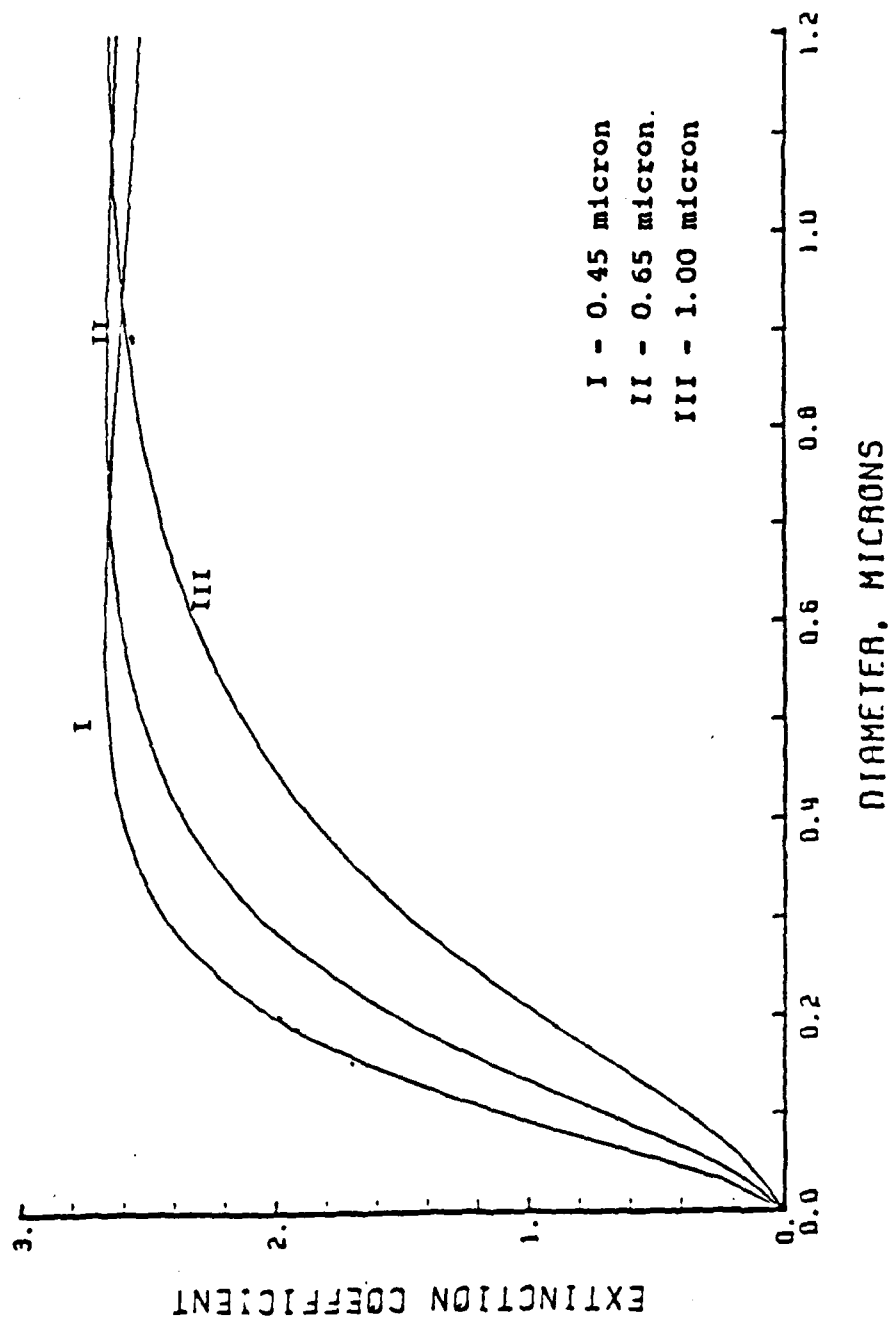


Figure 1. Extinction Coefficient versus D32

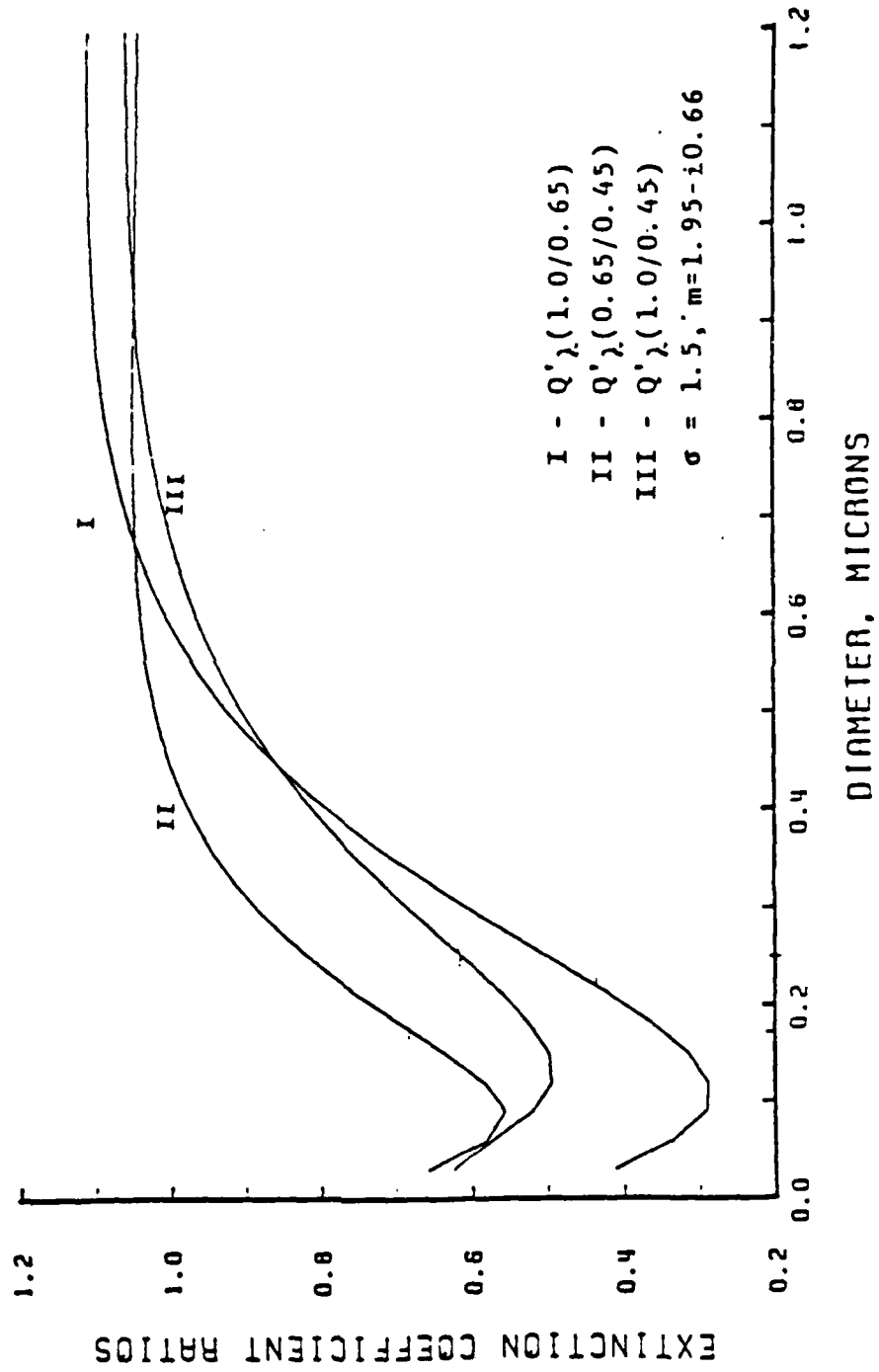


Figure 2. Extinction Coefficient Ratios versus D32

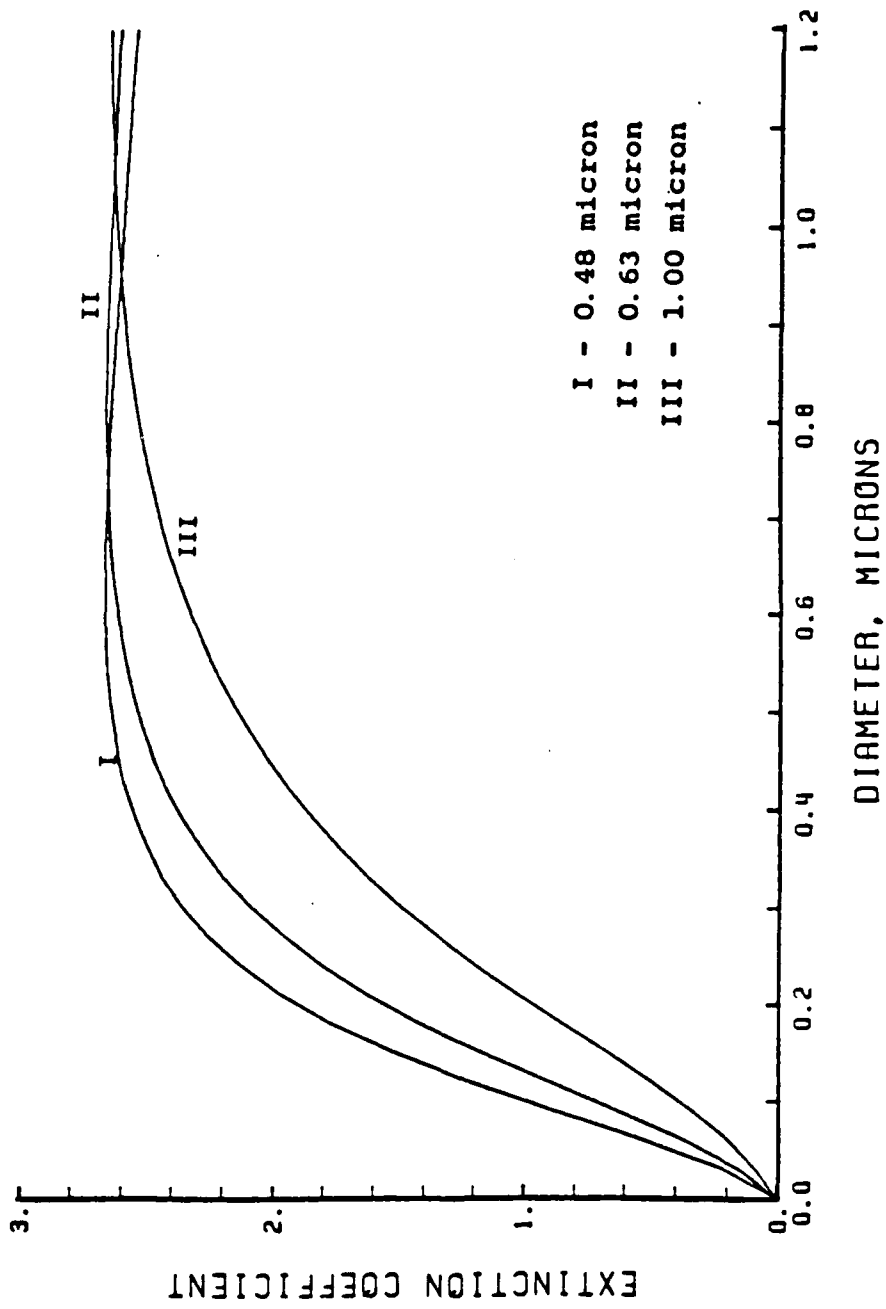


Figure 3. Extinction Coefficient versus D32

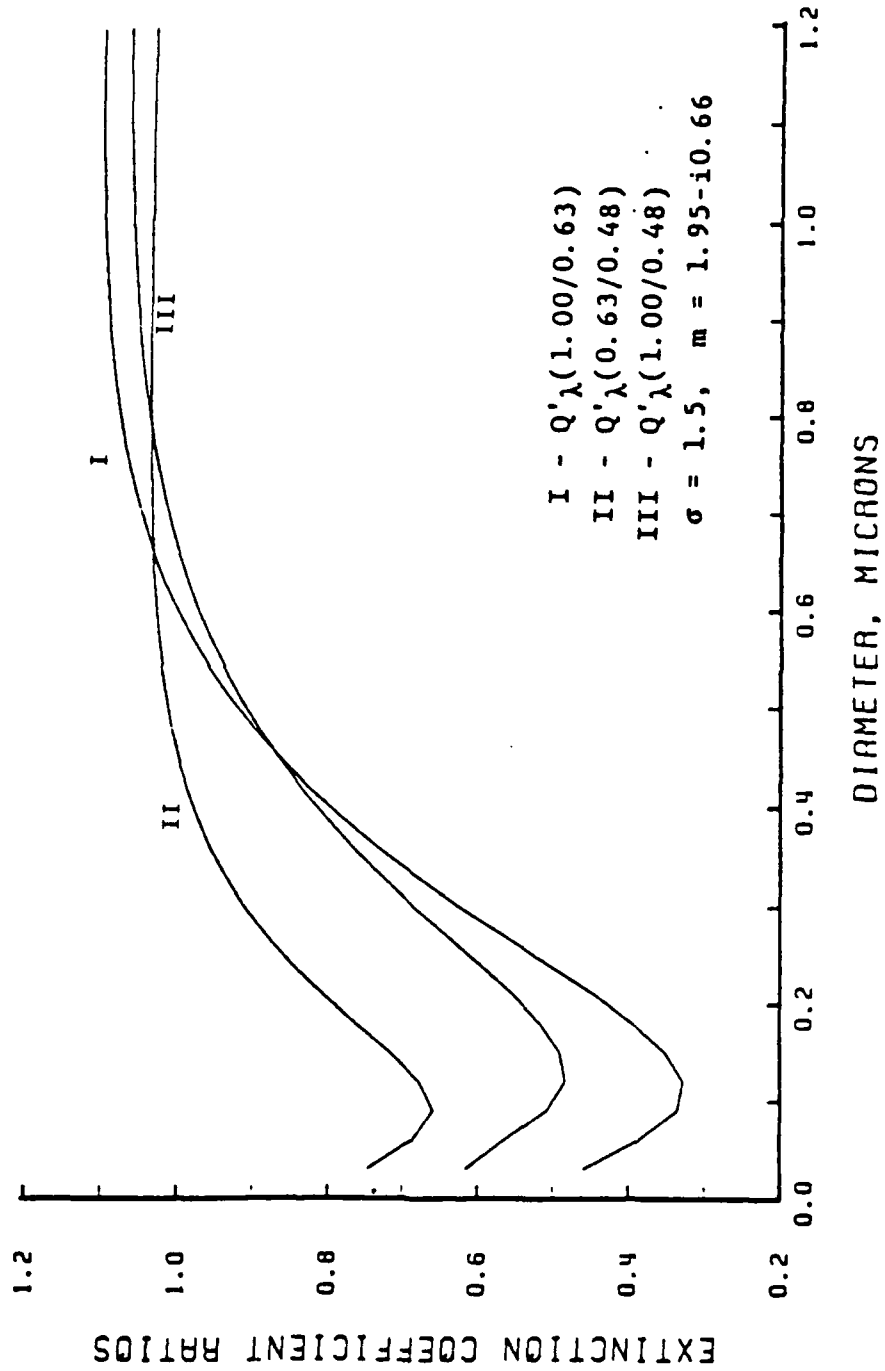
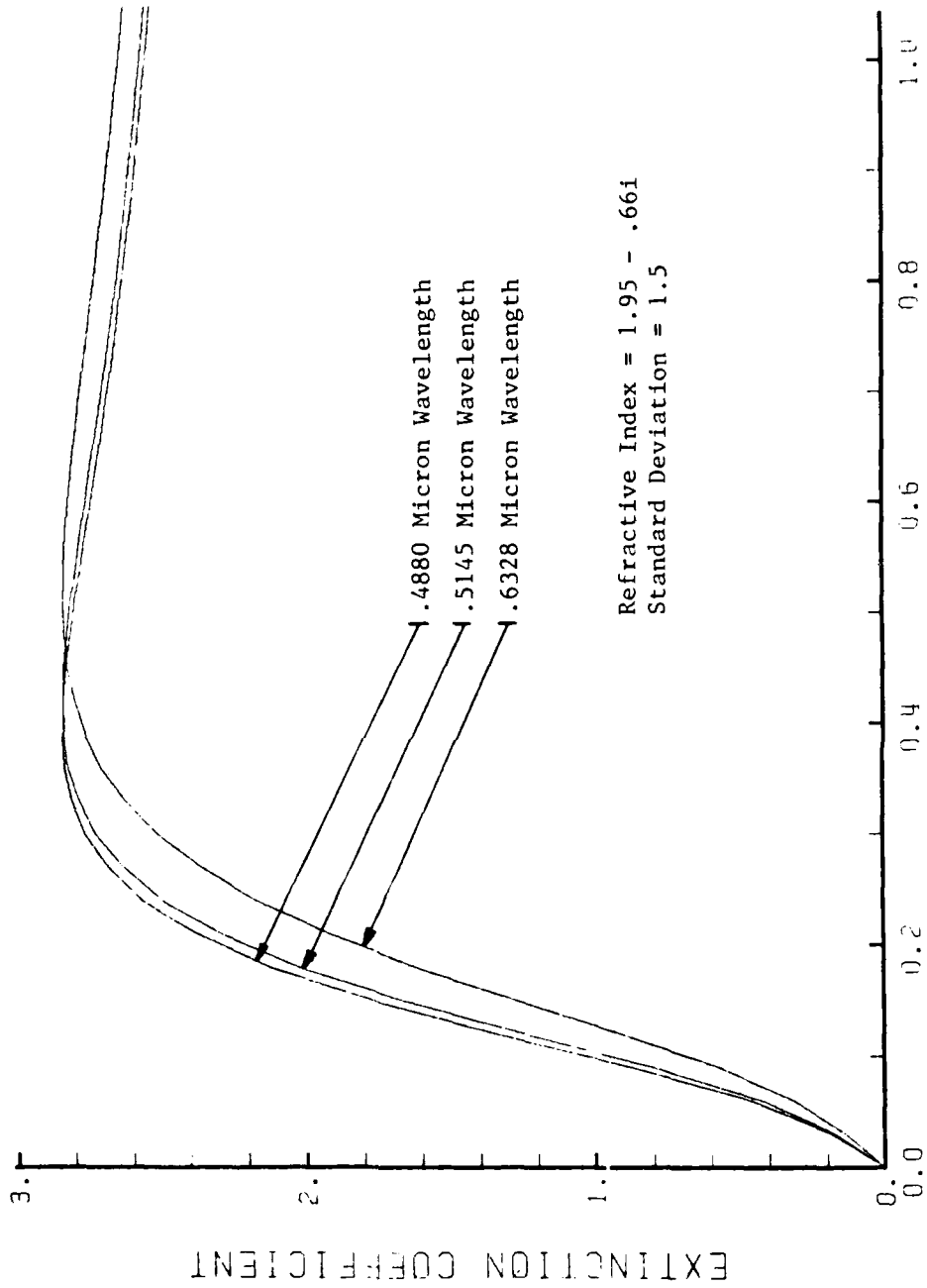


Figure 4. Extinction Coefficient Ratios versus D32



DIAMETER, MICRONS

FIGURE 5. EXTINCTION COEFFICIENT VS. PARTICLE SIZE (D₃₂)

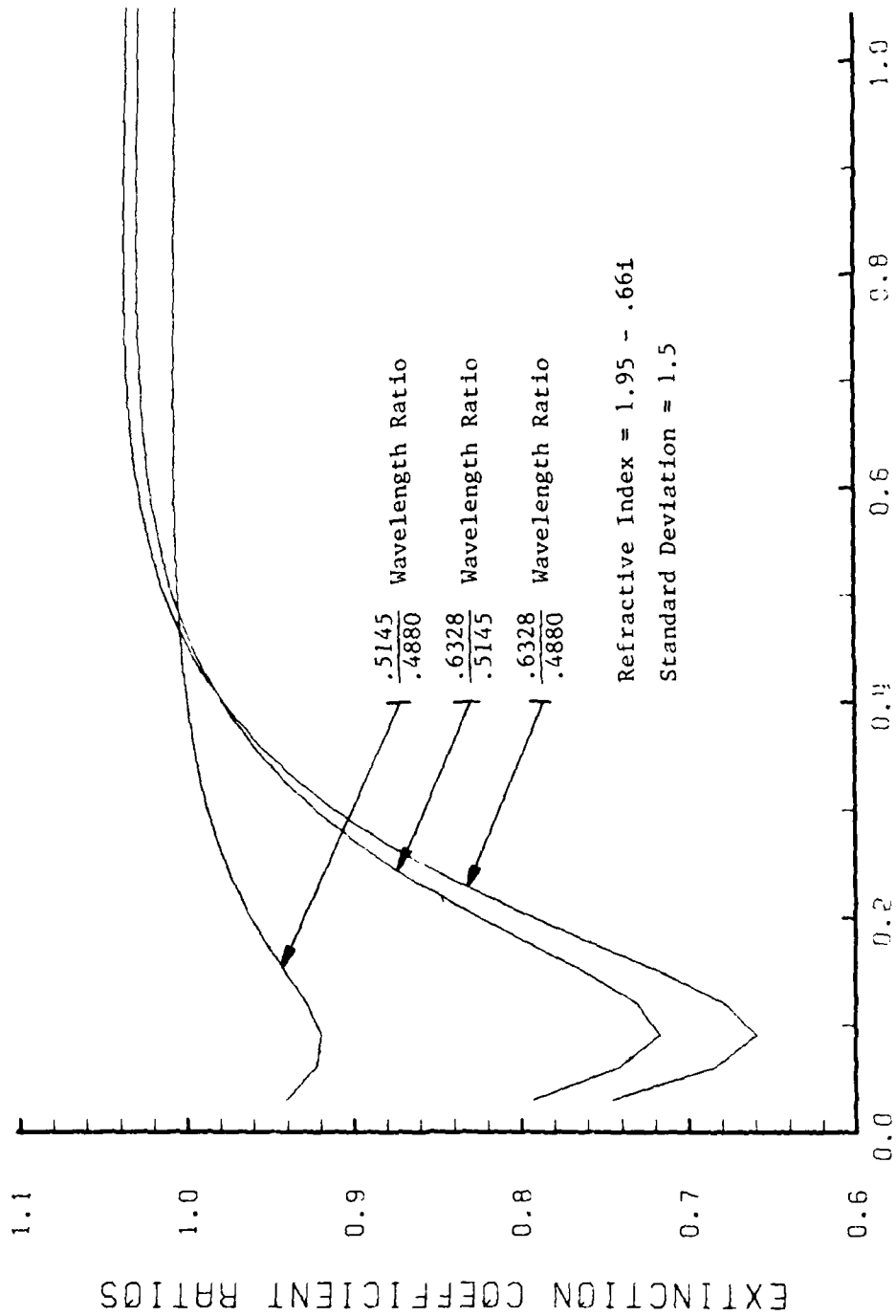


FIGURE 6. EXTINCTION COEFFICIENT RATIO VS. PARTICLE SIZE (D32)

PARTICLE SIZING USING SCATTERING
 .6328 MICRON WAVELENGTH

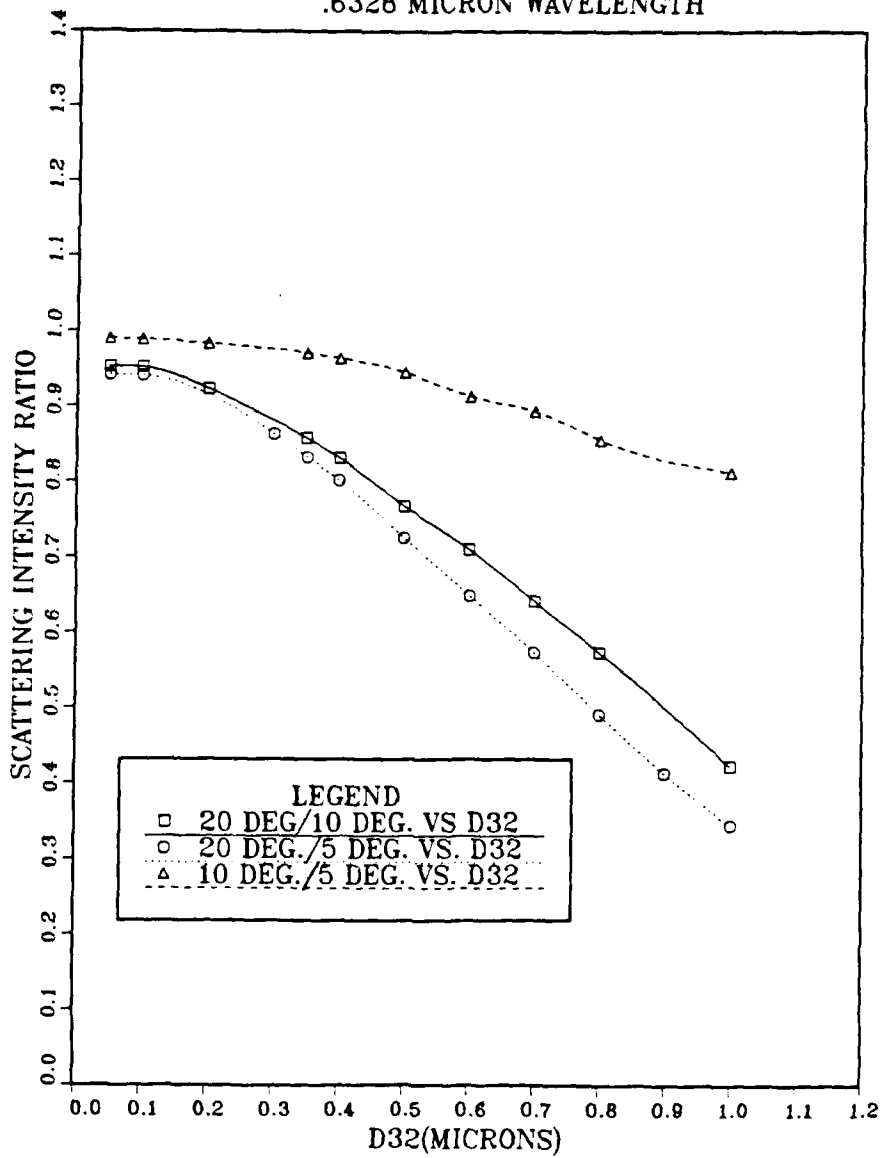


FIGURE 7. INTENSITY RATIO VERSUS D32

PARTICLE SIZING USING SCATTERING
.6328 MICRON WAVELENGTH

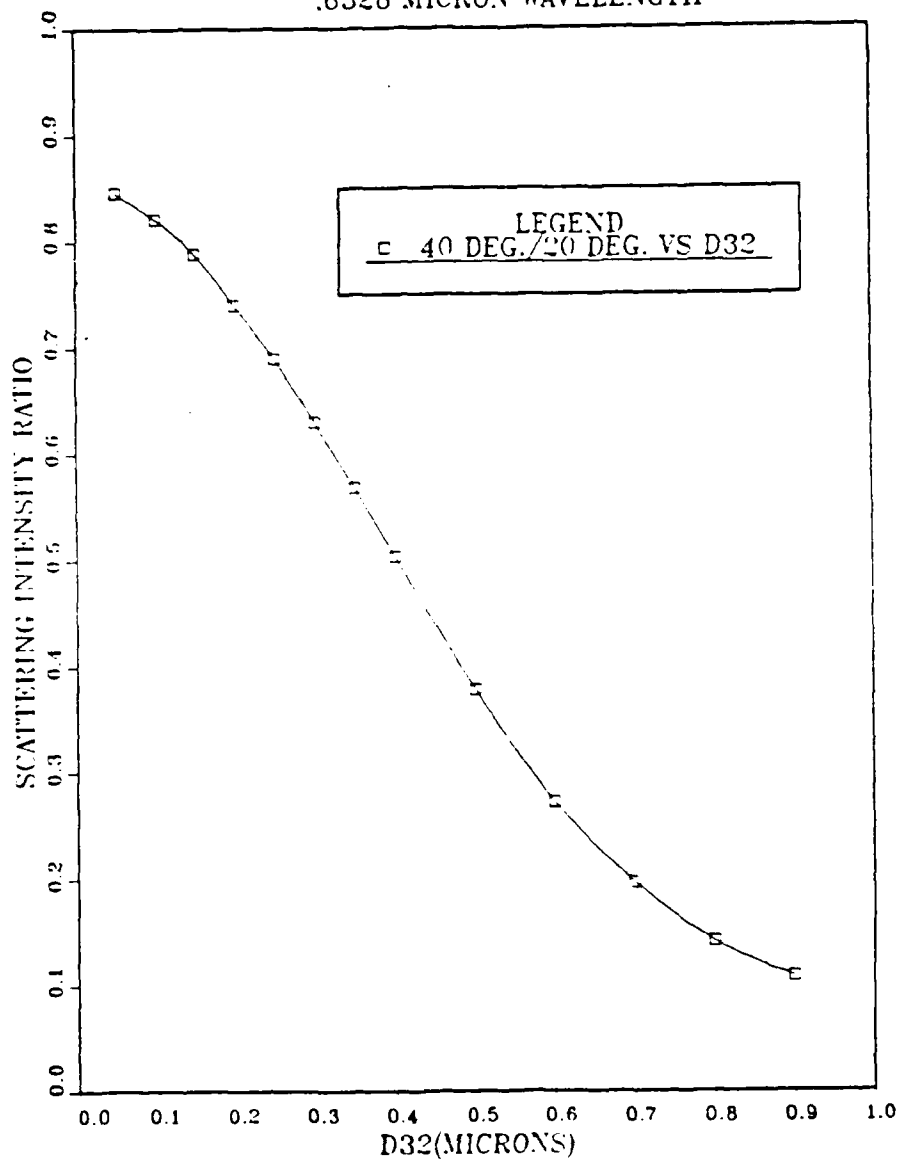


FIGURE 8. INTENSITY RATIO VERSUS D_{32}

PARTICLE SIZING USING SCATTERING
.4880MICRON WAVELENGTH LIGHT

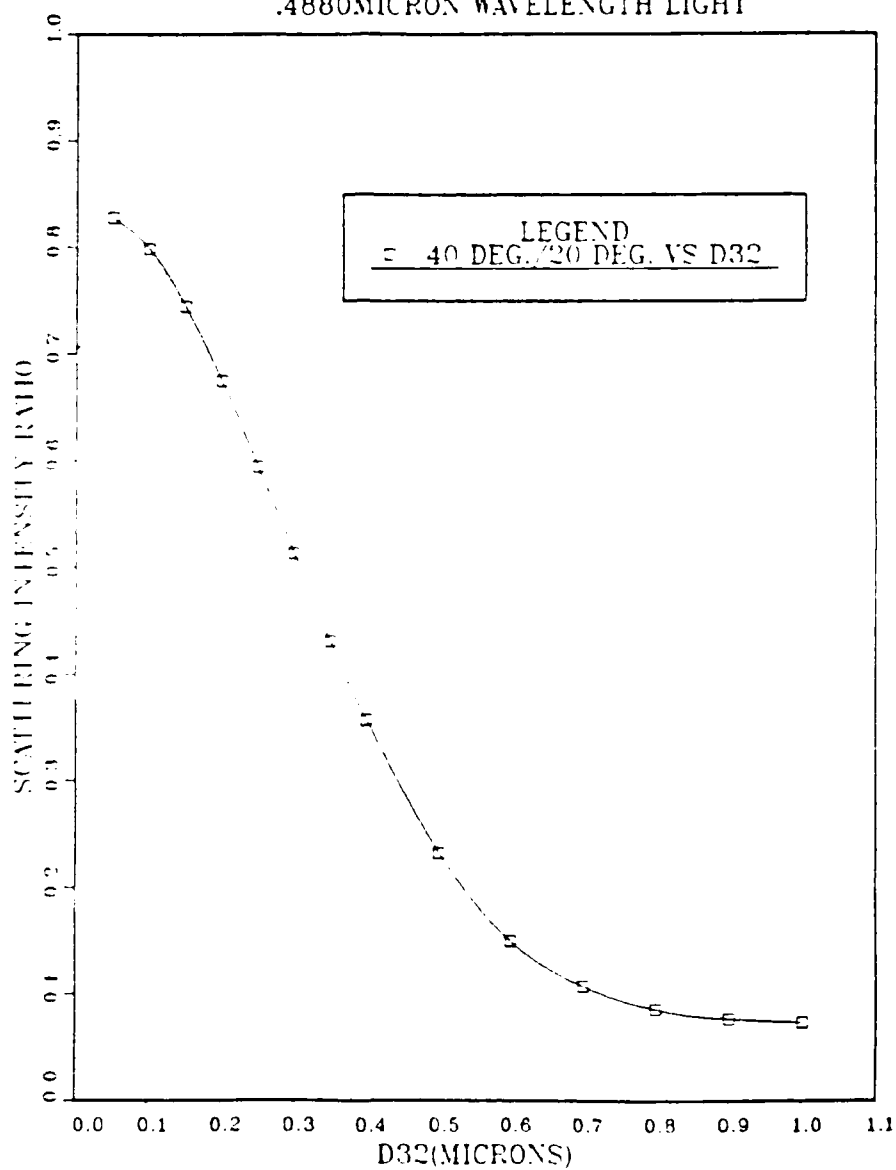


FIGURE 9. INTENSITY RATIO VERSUS D_{32}

PARTICLE SIZING USING SCATTERING
.6328 MICRON WAVELENGTH

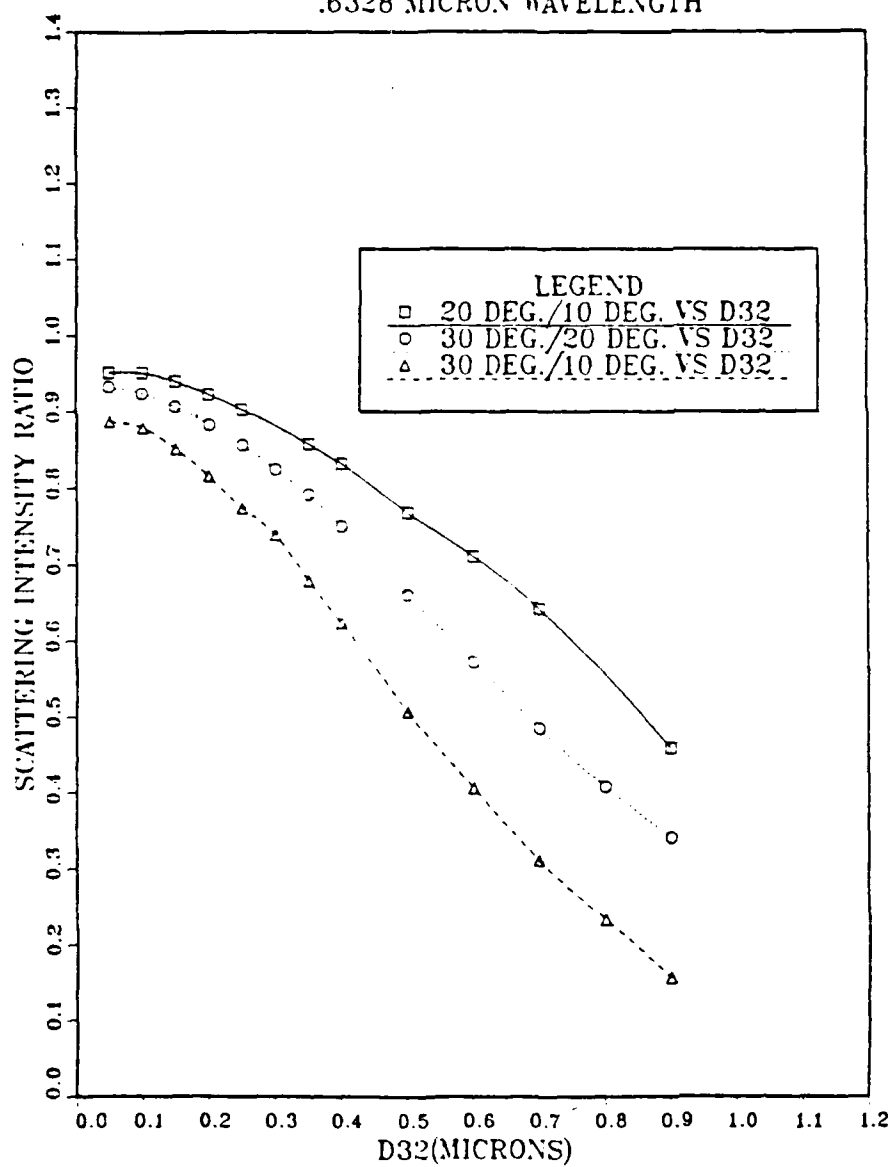


FIGURE 10. INTENSITY RATIO VERSUS D_{32}

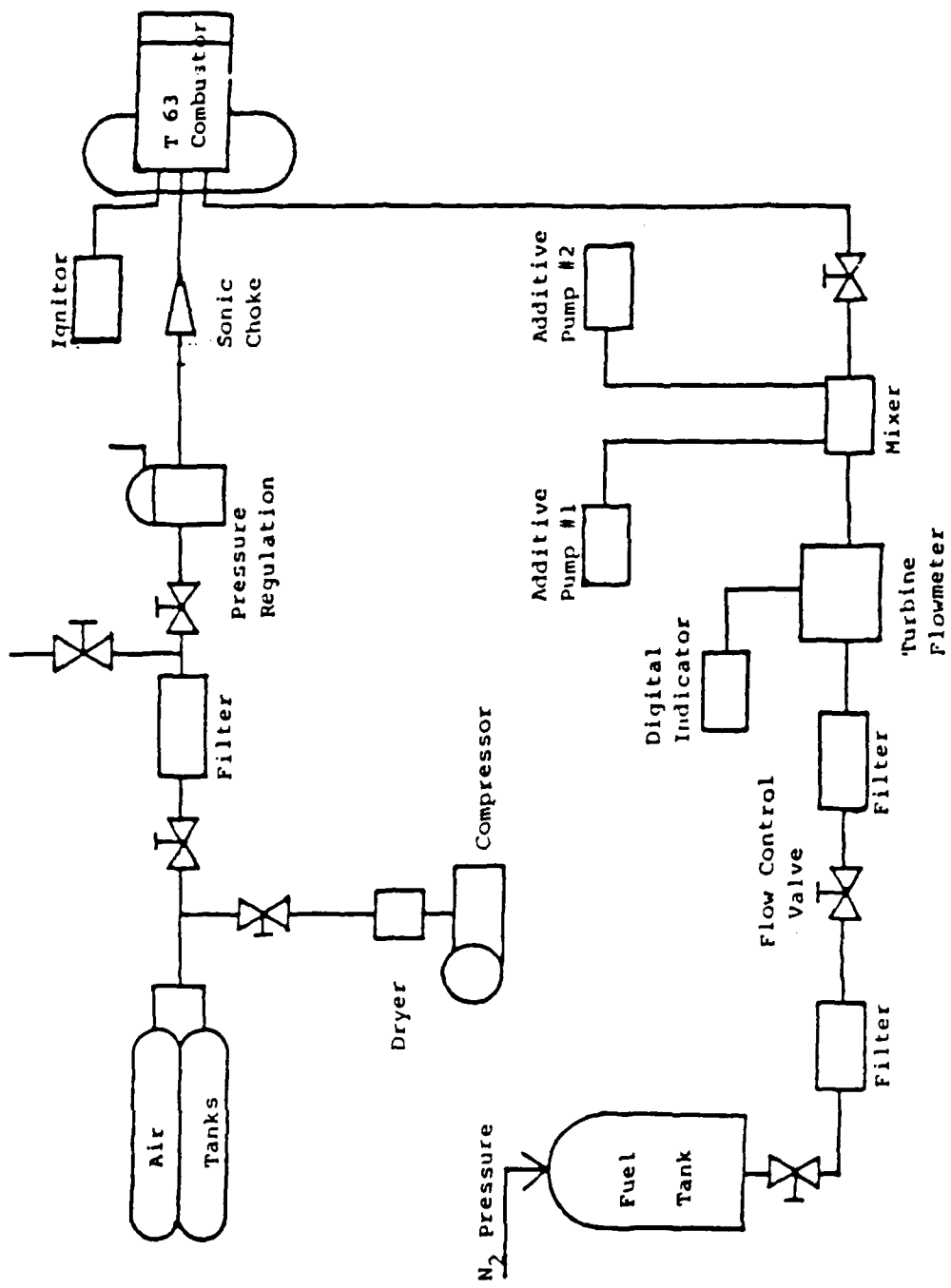


Figure 11. T-63 System Schematic [Ref. 1]

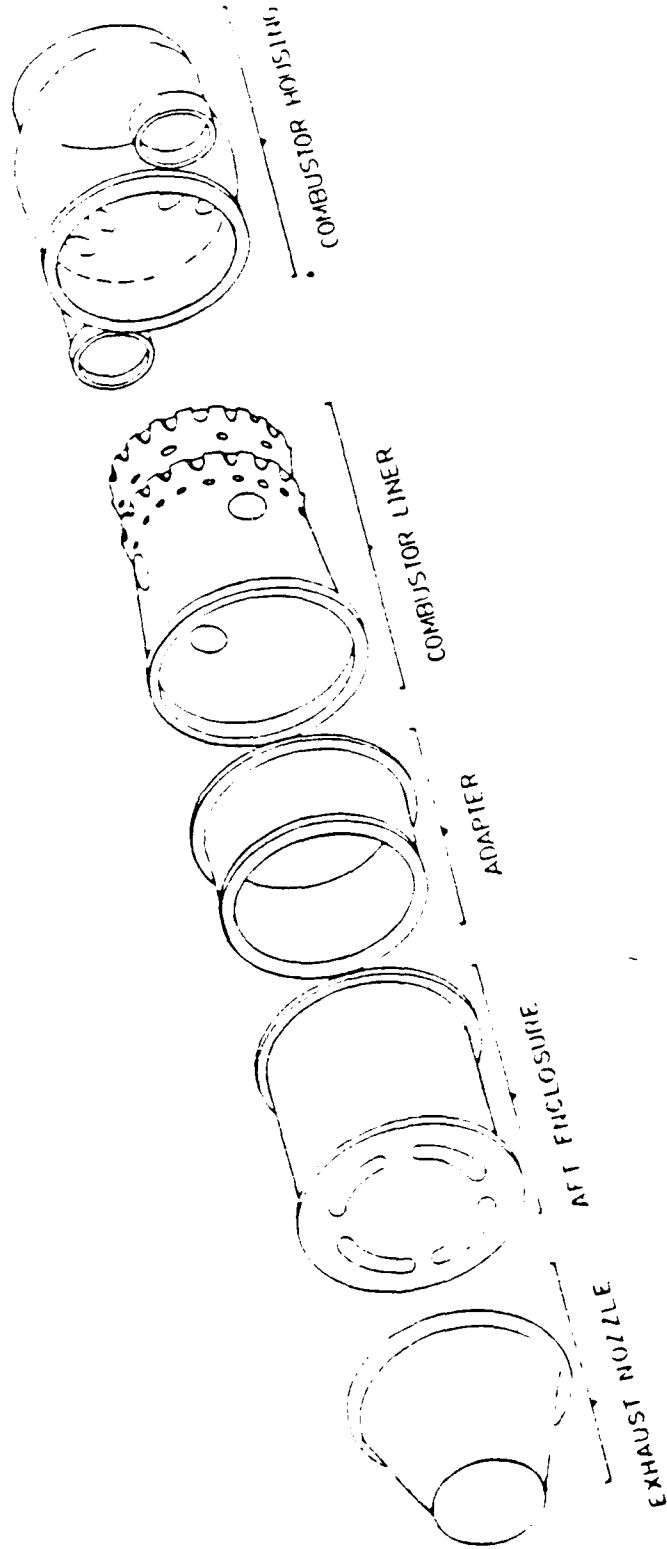


FIGURE 12. T-63 COMBUSTOR SCHEMATIC

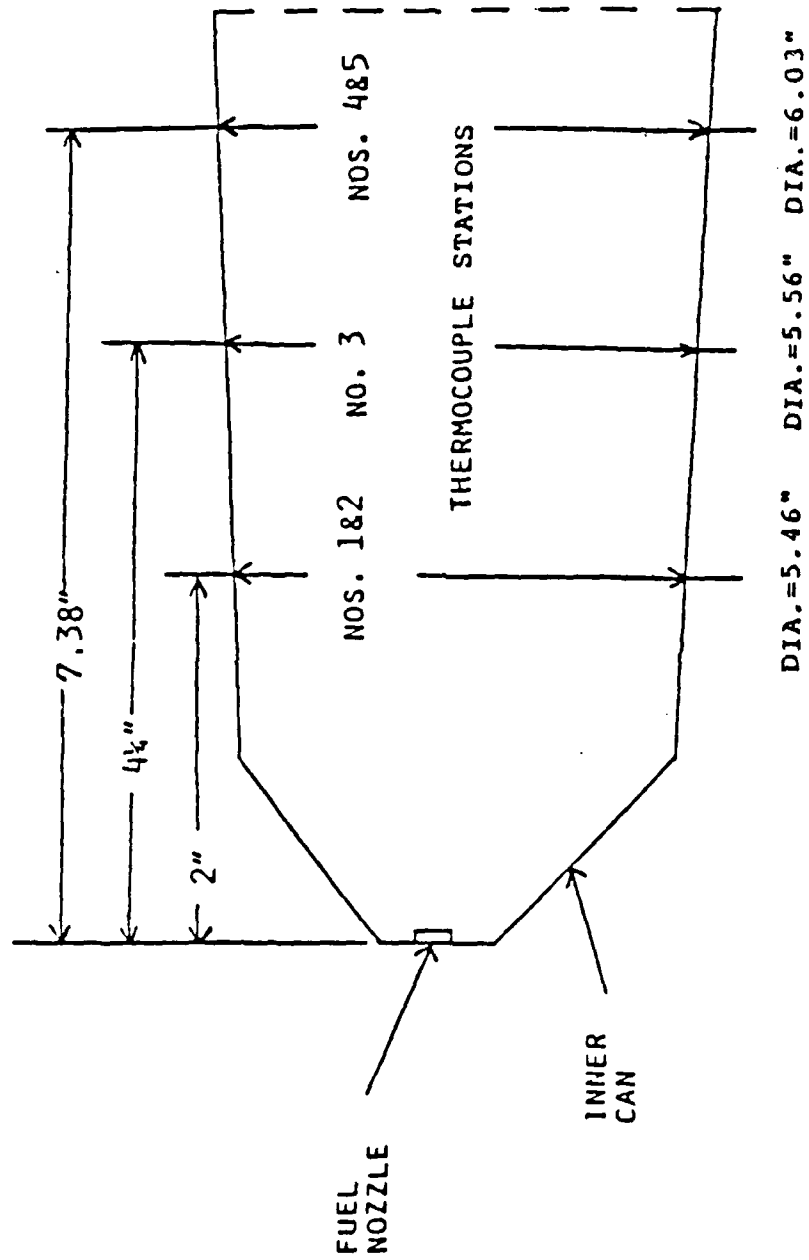
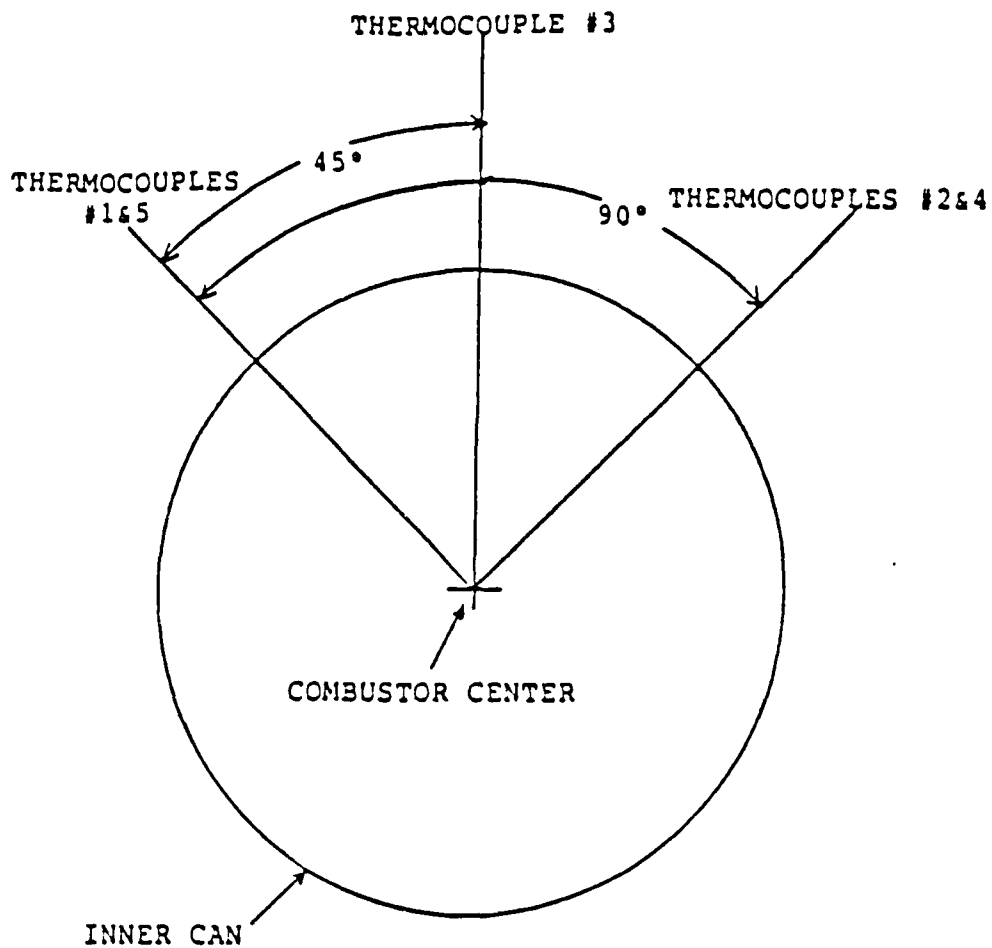


Figure 13. Side View of T-36 Thermocouple Locations [Ref. 1]



DISTANCE OF THERMOCOUPLES FROM COMBUSTOR CENTER

#1	2.23"
#2	1.73"
#3	2.28"
#4	2.01"
#5	NOT USED

Figure 14. End View of T-63 Thermocouple Locations [Ref. 1]

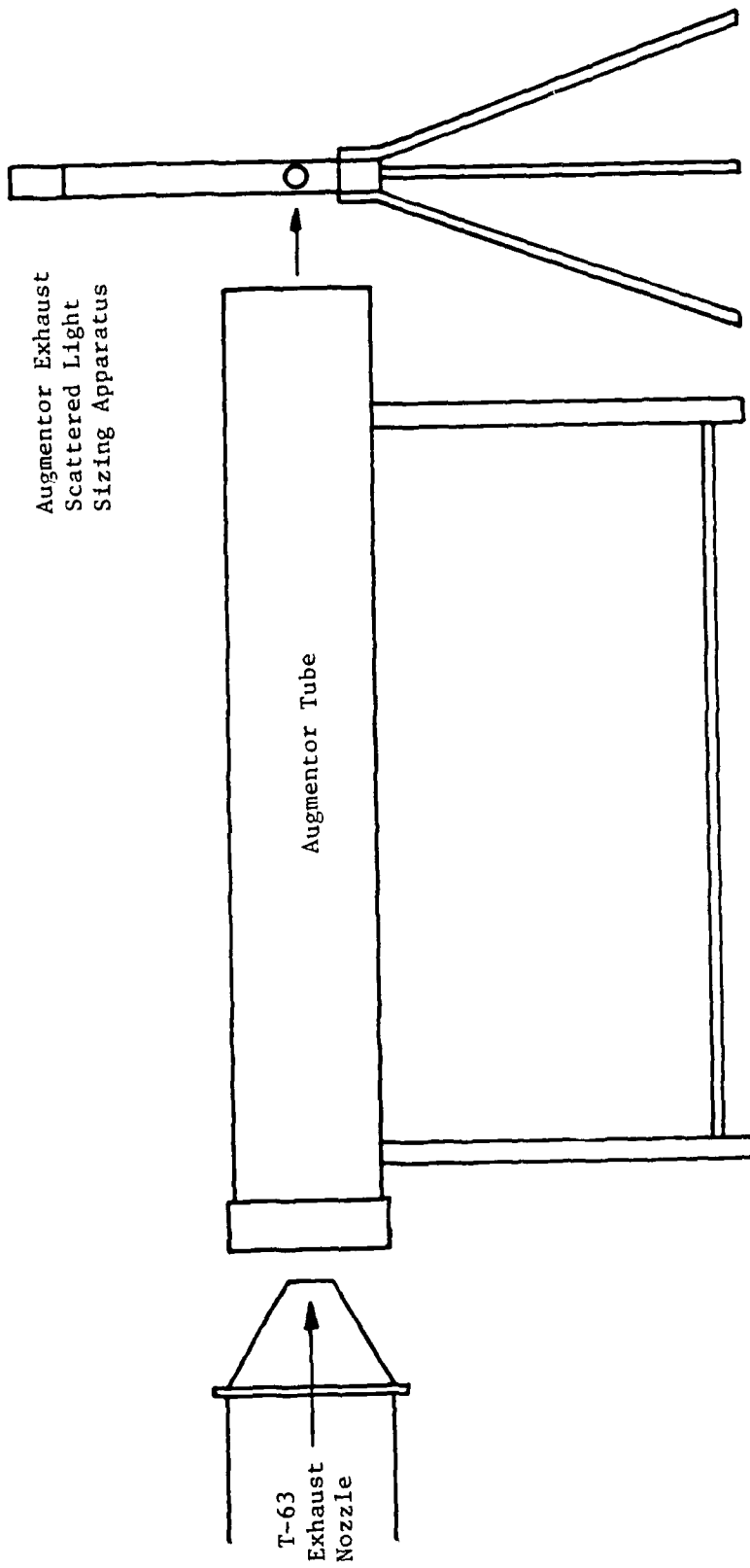


FIGURE 15. SCHEMATIC OF T-63 AUGMENTOR TUBE APPARATUS

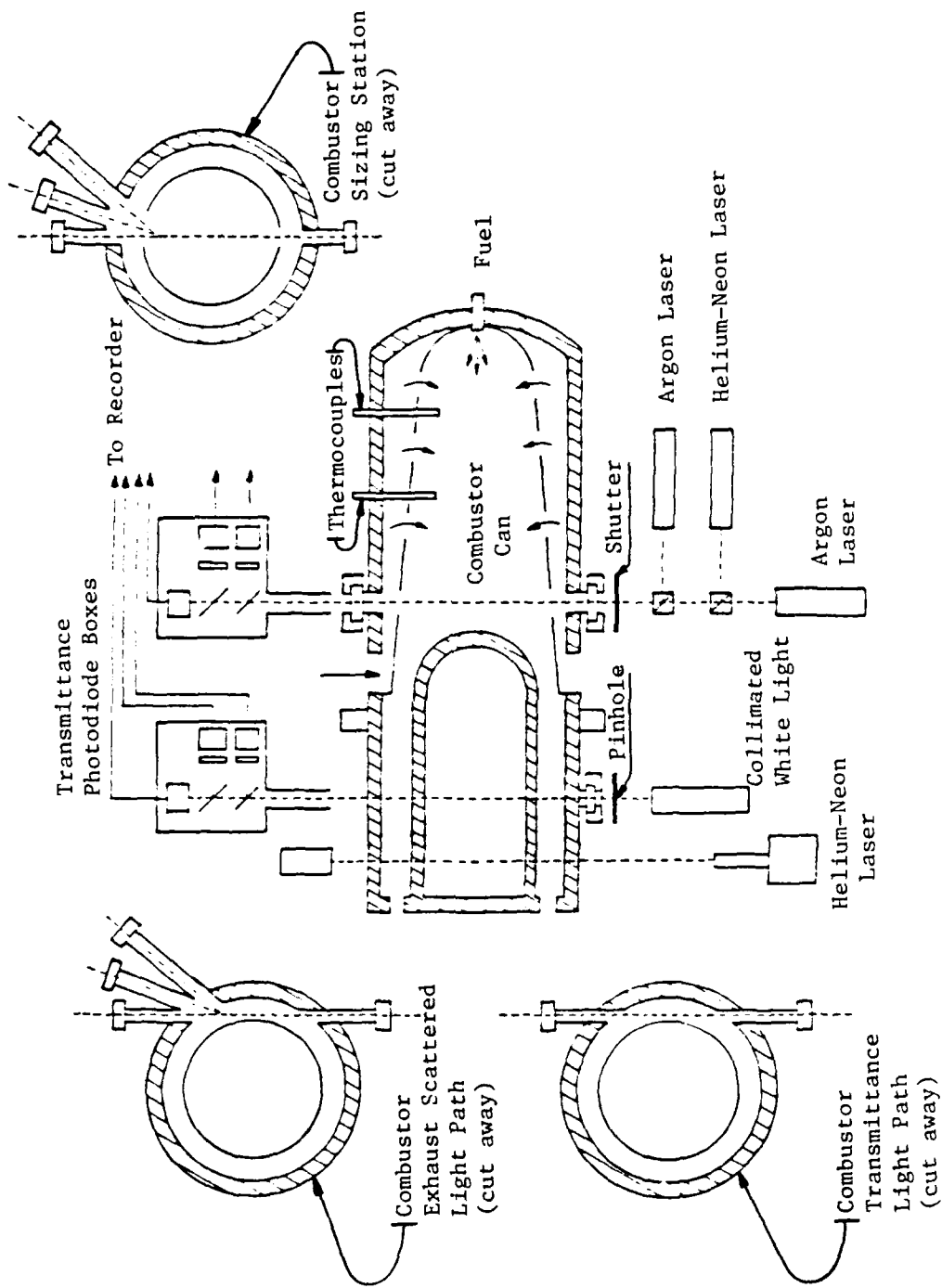


FIGURE 16. SCHEMATIC OF T-63 TEST APPARATUS (Adapted from Ref. 1)

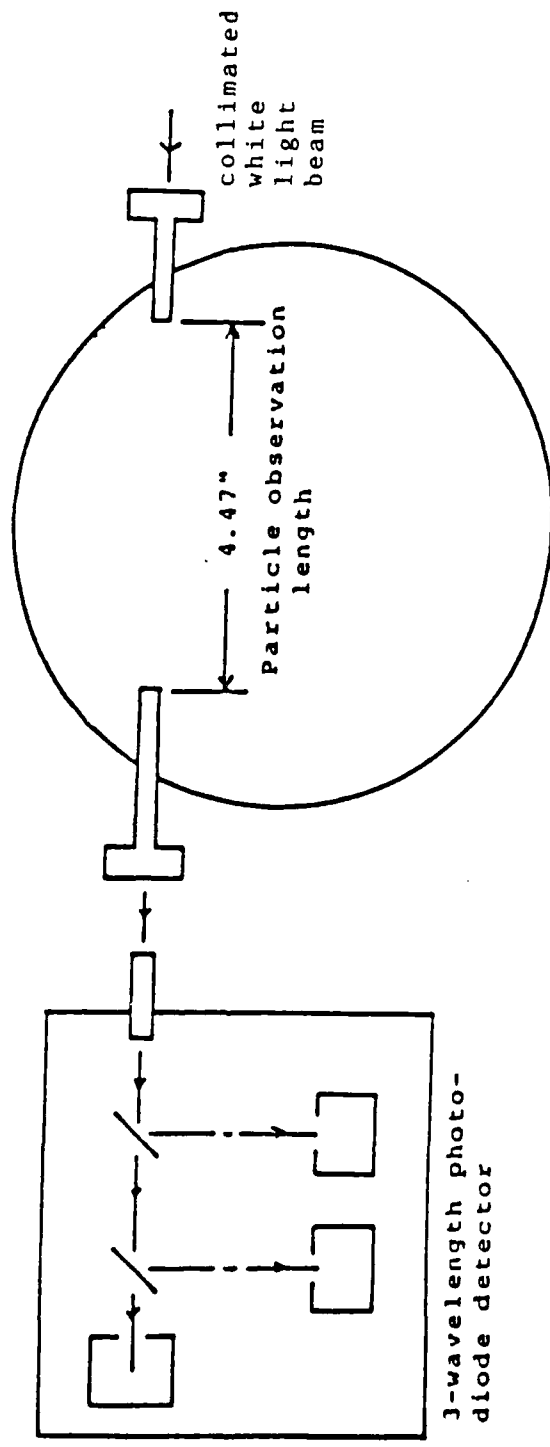


Figure 17. Schematic of T-63 Aft Can Transmittance Apparatus (Adapted from [Ref. 1])

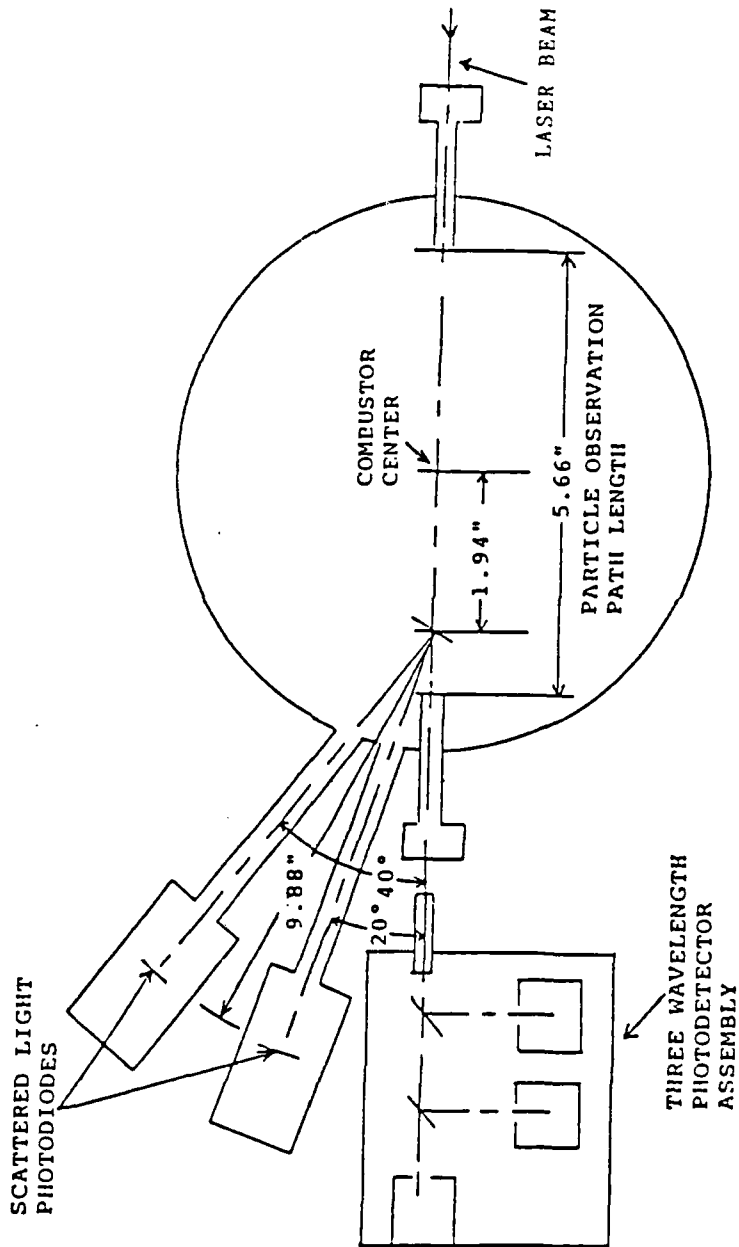


Figure 18. Schematic of T-63 Combustor Transmittance and Light Scattering Apparatus (Adapted from [Ref. 1])

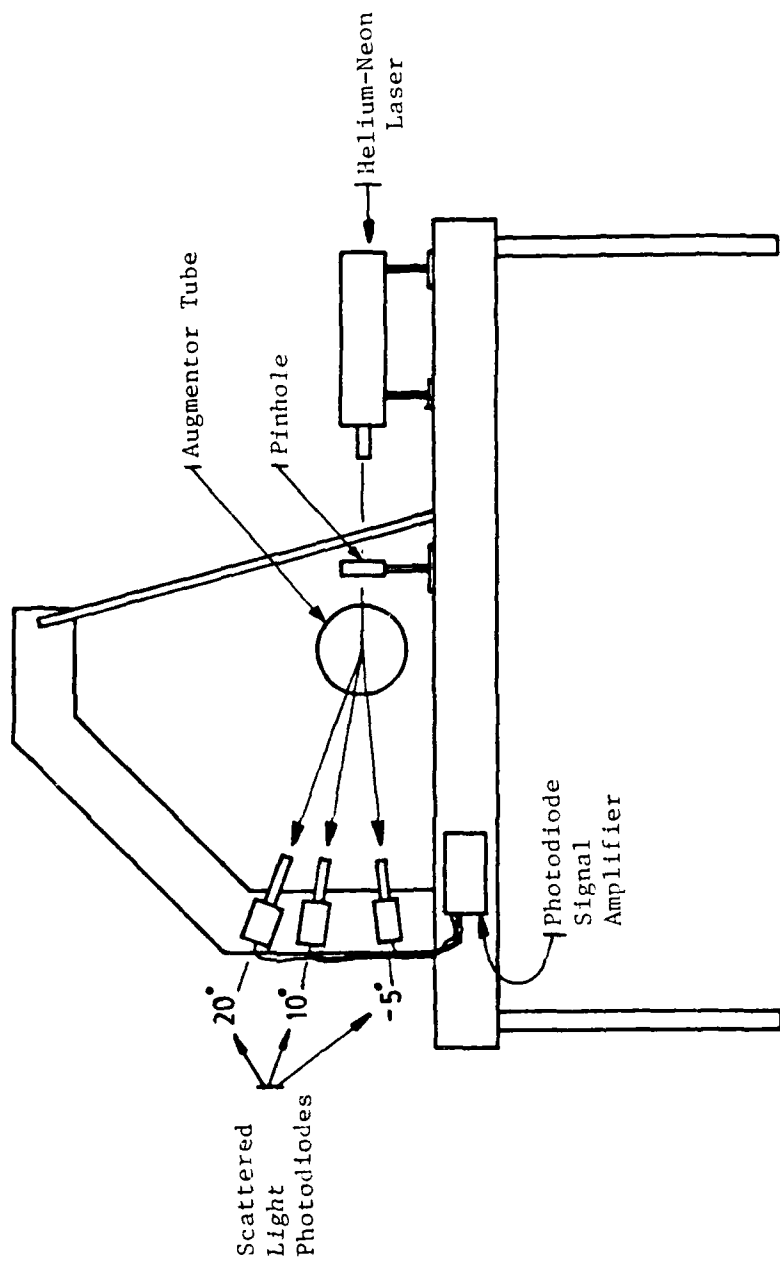


FIGURE 19. SCHEMATIC OF AUGMENTOR TUBE PARTICLE SIZING APPARATUS (END VIEW)

Malvern Instruments MASTER Particle Sizer M3.0 Date 25-02-87 Time 14-32

Size microns	under	in band	%	Size microns	under	in band	%	Result source=Sample
118.4	100.0	1.7	11.1	83.2	0.0	0.0	Record No. = 0	
102.1	98.3	4.0	9.6	83.2	0.0	0.0	Focal length = 63 mm.	
88.1	94.4	4.8	8.3	83.2	0.0	0.0	Experiment type pia	
76.0	89.5	4.2	7.2	83.2	0.0	0.0	Number distribution	
65.6	85.3	2.1	5.2	83.2	0.0	0.0	Beam length = 75.0 mm.	
56.6	83.2	0.0	5.3	83.2	0.0	0.0	Obscuration = 0.0523	
48.8	83.2	0.0	4.6	83.2	0.0	0.0	Volume Conc. = 0.0021 %	
42.1	83.2	0.0	4.0	83.2	0.0	0.0	Leq. Diff. = 6.10	
36.3	83.2	0.0	3.4	83.2	0.0	0.0	Model indp	
31.3	83.2	0.0	3.0	83.2	0.0	0.0	D(v, 0.5) = 1.7 µm	
27.0	83.2	0.0	2.6	83.2	0.0	0.0	D(v, 0.9) = 77.1 µm	
23.3	83.2	0.0	2.2	83.2	0.1	0.1	D(v, 0.1) = 1.6 µm	
20.1	83.2	0.0	1.9	83.1	60.6	60.6	D(4, 3) = 14.9 µm	
17.4	83.2	0.0	1.6	22.5	20.0	20.0	D(3, 2) = 1.9 µm	
15.0	83.2	0.0	1.4	2.6	0.0	0.0	Span = 43.7	
12.9	83.2	0.0	1.2	2.6	0.2	0.2	Spec. surf. area = 0.07 sq. m. / cc.	

Sample details: -Test data 03-06-1986. R. J. H. J.

Figure 20. MALVERN Particle Size Data for Augmentor Tube Exit

Malvern Instruments MASER Particle Sizer M3.0 Date 25-02-07 Time 15-10

Size microns	under	% in band	Size microns	under	% in band	Result source=Sample Record No. = 0
110.4	100.0	0.0	11.1	99.8	0.0	Focal length = 63 mm.
102.1	100.0	0.0	9.6	99.8	0.0	Experiment type pia
88.1	100.0	0.0	8.3	99.8	0.0	Number distribution
76.0	100.0	0.1	7.2	99.8	0.0	Beam length = 51.0 mm.
65.6	99.9	0.1	6.2	99.8	0.0	Obscuration = 0.0218
56.6	99.8	0.0	5.3	99.8	0.0	Volume Conc. = 0.0009 %
48.8	99.8	0.0	4.6	99.8	0.0	Log. Diff. = 5.73
42.1	99.8	0.0	4.0	99.7	0.0	Model indep
36.3	99.8	0.0	3.4	99.7	0.2	D(V, 0.5) = 1.2 µm
31.3	99.8	0.0	3.0	99.6	0.2	D(V, 0.2) = 1.4 µm
27.0	99.8	0.0	2.6	99.4	0.2	D(V, 0.1) = 1.0 µm
23.3	99.8	0.0	2.2	99.2	0.6	D(4, 3) = 1.4 µm
20.1	99.8	0.0	1.9	98.6	1.5	D(3, 2) = 1.2 µm
17.4	99.8	0.0	1.6	97.1	10.1	Span = 0.3
15.0	99.8	0.0	1.4	87.0	41.7	Spec. surf. area
12.9	99.8	0.0	1.2	45.3	41.4	0.07 sq. m./cc.

Sample details:-Test data 03-06-1986. R.J.H.J.

Figure 21. MALVERN Particle Size Data for Exhaust Nozzle

LIST OF REFERENCES

1. Bennett, J.S., Jway, C.H., Urich, D.J., and Netzer, D.W., "Gas Turbine Combustor and Engine Augmentor Tube Sooting Characteristics," Naval Postgraduate School, Monterey, California, December 19086, NPS Paper 67-86-004.
2. Cashdollar, K.L., Lee, C.K., and Singer, J.M., "Three Wavelength Light Transmission Techniques to Measure Smoke Particle Size and Concentration," Applied Optics, Vol. 18, No. 18, pp. 1763-1769, June 1979.
3. Dobbins, R.A. and Jizmagian, G.S., "Measurement of Mean Particle Size of Sprays from Diffractively Scattered Light," AIAA Journal, Vol. 1, No. 8m pp. 1882-1886, August 1963.
4. Powell, E.A., Cassanova, R.A., Bankston, C.P., and Zinn, B.T., "Combustion Generated Smoke Diagnostics by Means of Optical Measurement Techniques," AIAA 14th Aerospace Sciences Meeting, January 1976, AIAA Paper No. 76-67.
5. Powell, E.A. and Zinn, B.T., "In Situ Measurement of the Complex Refractive Index of Combustion Generated Particulates," AIAA 18th Thermophysics Conference, June 1983, AIAA Paper 83-1516.
6. Lohman, A.L., An Investigation into the Soot Production Process in a Gas Turbine Engine, Master's Thesis, Naval Postgraduate School, September 1984.

INITIAL DISTRIBUTION LIST

	NO. OF COPIES
1. Library Code 0142 Naval Postgraduate School Monterey, CA 93943	2
2. Department of Aeronautics Code 67 Naval Postgraduate School Monterey, CA 93943-5000 - Chairman - D. W. Netzer	1 10
3. Research Administration Code 012 Naval Postgraduate School Monterey, CA 93943-5000	1
4. Defense Technical Information Center Cameron Station Alexandria, VA 22314	2
5. Chief of Naval Operations Navy Department Washington, D.C. 20360 (Attn: Code OP451, IP453)	2
6. Chief of Naval Material Navy Department Washington, D.C. 20360 (Attn: Codes: 08T241, 044P1)	2
7. Commander Naval Air Systems Command Washington, D.C. 20360 (Codes: AIR-01B, 330D, 3407, 4147A, 50184, 5341B, 53645, 536B1)	8
8. Commanding Officer Naval Air Rework Facility Naval Air Station North Island San Diego, CA 92135	1
9. Commander Naval Facilities Engineering Command 200 Stoval Street Alexandria, VA 22332 (Codes: 104, 032B)	2

INITIAL DISTRIBUTION LIST

	NO. OF COPIES
10. Naval Construction Battalion Center Port Hueneme, CA 93043 (Codes: 25, 251, 252)	3
11. U.S. Naval Academy Annapolis, MD 21402 (Attn: Prof. J. Williams)	1
12. Arnold Engineering Development Center Arnold AFB, TN 37342 (Code: DYR)	1
13. Air Force Aero Propulsion Laboratory Wright-Patterson AFB, OH 45433 (Code: SFF)	1
14. Detachment 1 (Civil & Environmental Engineering Division Office) HQ ADTC (AFSC) Tyndall AFB, FL 32401 (Codes: EV, EVA)	2
15. Army Aviation Systems Command P. O. Box 209 St. Louis, MO 63166 (Code: EQP)	1
16. Eustis Directorate USA AMR & DL Ft. Eustis, VA 23604 (Code: SAVDL-EU-TAP)	1
17. National Aeronautics and Space Administration Lewis Research Center 2100 Brookpark Road Cleveland, OH 44135 (Attn: Mail Stop 60-6 (R. Rudley))	1
18. Federal Aviation Administration National Aviation Facility Experimental Ctr. Atlantic City, NJ 08405	1
19. Naval Air Propulsion Center Trenton, NJ 08628-0176 (Code: Pe 71:AFK)	3

INITIAL DISTRIBUTION LIST

NO. OF COPIES

20. Naval Ocean Support Center
271 Catalina Boulevard
San Diego, CA 92152
(Attn: M. Lepor, M. Harris, Code 5121)

2

21. Naval Air Rework Facility
Alameda, CA 94501
(Attn: G. Evans, Code 642)

1